

Fast Radio Bursts and cosmological tests

M. Jaroszynski^{1*}

¹University of Warsaw Observatory, Al. Ujazdowskie 4, 00-478 Warsaw, Poland

Accepted; Received ;

ABSTRACT

We consider future cosmological tests based on observations of Fast Radio Bursts (FRBs). We use Illustris Simulation to realistically estimate the scatter in the dispersion measure (DM) of FRBs caused by the inhomogeneous distribution of ionized gas in the Intergalactic Medium (IGM). We find $\sim 13\%$ scatter in DM to a source at $z = 1$ and $\sim 7\%$ at $z = 3$ (one sigma). The distribution of DM is close to Gaussian. We simulate samples of FRBs and examine their applicability to simple cosmological tests. Our calculations show that using a sample of 100 FRBs and fixing cosmological model one can find the redshift and sample averaged fraction of ionized gas with $\sim 1\%$ uncertainty. Finding the ionized fraction with $\sim 1\%$ accuracy at few different epochs would require $\sim 10^4$ FRBs with known redshifts. Because DM is proportional to the product of ionized fraction, baryon density and the Hubble constant it is impossible to constrain these parameters separately with FRBs. Constraints on cosmological densities are possible in a flat Λ CDM model but give uninterestingly low accuracy. Using FRBs with other type of data improves the constraints, but the role of FRBs is not crucial. Thus constraints on the distribution of ionized gas are probably the most promising application of FRBs which allow for "tomography" if sources redshifts are known, as opposed to measuring τ_e or y parameters with CMB observations.

Key words: radio continuum: transients – cosmological parameters

1 INTRODUCTION

The discovery of fast radio bursts (FRBs) (Lorimer et al. 2007), large dispersion measures (DM) of some of them (Tendulkar et al. 2017), and measured redshifts (Chatterjee et al. 2017; Tendulkar et al. 2017) make them a class of phenomena which (at least in part) may be happening at cosmological distances. Their application to cosmological tests has been proposed by several authors (Zhou et al. 2014; Gao, Li & Zhang 2014; Lorimer 2016; Yu and Wang 2017), to cite few.

In a recent article (Ravi 2017) the properties of known FRBs are discussed. They seem to be a nonuniform class of objects with complicated characteristics and the extragalactic origin of DM is likely only in a part of the sources. The number of known FRBs is far too low to study their distribution on the sky or make a meaningful $\lg F - \lg N$ test, which could disprove the cosmological hypothesis (compare Paczynski 1995 for the case of gamma ray bursts and Katz 2017 for FRBs). We assume, that there is a cosmological population of FRBs and that the improved instruments (e.g. Square Kilometer Array) will allow to study a large number of these events.

Locally the observed DM is proportional to the column density of free electrons along the line of sight (LOS) to the source. It is precisely measured for pulsars (see e.g. Bilous et al. 2016). It is used to find distances to the sources independently of any *cosmic ladder*. DM measurements are based on the fact that lower fre-

quency radio signals travel with lower velocities in plasma, so they are delayed as compared to a higher frequency signals. The delay can be measured. In an expanding universe the contributions from free electron column density at small redshift interval $z - z + \Delta z$ scale with the redshift factor as $\propto 1/(1+z)$. On the other hand one can expect the density of free electrons $n_e \propto (1+z)^3$ which makes the contributions from high redshift dominating. Thus there is no direct proportionality between DM and the proper distance to the source even in an uniform universe.

Shull & Danforth (2018) model the distribution of free electrons in space based on the observations of absorption lines in QSO spectra and the relations between the neutral and ionized fractions of the gas at different redshifts. They also estimate the redshifts of the known FRBs using a uniform flat universe model, showing that in five of twenty five considered cases $z > 1$.

We are simulating cosmological tests based on possible future samples of FRBs with known dispersion measures and redshifts. In our approach we calculate DM along many LOS to distant sources employing the results of the Illustris Simulation (Vogelsberger et al. 2014a,b) which are publicly available (Nelson et al. 2015) and give the spatial distribution of ionized gas for a discrete set of redshifts. Cosmological simulations were used in the past by McQuinn (2014) to estimate the variance of the dispersion measure due to the inhomogeneity of the gas distribution in space and by Dolag et al. (2015), who considered various aspects of FRBs including the large scale structure influence on the derived properties of sources population.

* E-mail: mj@astrouw.edu.pl

In the next section we describe our method to calculate DM to a source at given redshift using Illustris data. In Sec. 3 we describe a possible cosmological test based on a simulated sample of a hundred FRBs with measured hosts redshifts, concentrating on possible estimates of the fraction of ionized gas in space. In Sec. 4 we use the SN Ia *Union* sample [Kowalski et al. 2008](#) to investigate the role of other data on the applicability of FRBs to cosmological tests. Discussion follows in the last section.

2 CALCULATION OF THE DISPERSION MEASURE IN A NONUNIFORM UNIVERSE MODEL

2.1 The method

We are using the results of Illustris Simulation to describe the evolving ionized gas distribution in space. The Simulation provides the history of the structure formation in a cube of 75 Mpc/ h edge length, including the distribution of free electrons. To save the storage space and the calculations time we use Illustris-3, which has the lowest spatial resolution.

The dispersion measure for a source at the redshift z_S , neglecting the contribution from our Galaxy, the source itself, and its host galaxy, can be calculated as an integral along the path from the source to the observer (compare [Deng & Zhang 2014](#), [Zhou et al. 2014](#), [Gao, Li & Zhang 2014](#)):

$$DM(z_S) = \int_0^{z_S} \frac{n_e(z) dl_{\text{prop}}}{1+z} dz = \int_0^{z_S} \frac{c/H_0 n_e(z) dz}{(1+z)^2 h(z)} \quad (1)$$

where n_e is the concentration of free electrons along the LOS, dl_{prop} is the proper distance differential, z - the redshift, c - the speed of light, and $H_0 = 100 h$ km/s/Mpc - the Hubble constant. In a Λ CDM model:

$$h(z) = \sqrt{\Omega_M(1+z)^3 + \Omega_K(1+z)^2 + \Omega_\Lambda} \quad (2)$$

where Ω_M is the matter density parameter (baryons and dark matter), Ω_Λ - dark energy density parameter, $\Omega_K \equiv 1 - \Omega_M - \Omega_\Lambda$ - the curvature parameter, and $h(z) \equiv H(z)/H_0$ gives the rate of expansion as a function of z . DM here represents its inter-galaxy medium part (DM_{IGM}) but we omit this subscript for compactness. In Illustris the cosmological parameters have the following values (denoted by an extra "I" in the subscripts): $H_{0I} = 70.4$ km s $^{-1}$ Mpc $^{-1}$, $\Omega_{MI} = 0.2726$, $\Omega_{\Lambda I} = 0.7274$, and the baryon density parameter $\Omega_{BI} = 0.0456$.

rm The characteristic present number density of electrons in a uniform universe model with hydrogen and helium mass fractions X, Y , assuming complete ionization is given as:

$$n_{e0} = \left(X + \frac{1}{2}Y \right) \Omega_B \frac{3H_0^2}{8\pi G} \frac{1}{m_H} = 2.22 \times 10^{-7} \text{ cm}^{-3} \quad (3)$$

The numeric value is calculated for the Illustris model parameters with the primordial abundances $X = 0.75$ and $Y = 0.25$.

The averaged free electron concentration $\langle n_e \rangle$ in the IGM depends on the fraction of gas mass belonging to the IGM f_{IGM} , on the gas chemical composition, and the ionization state of all species. We use a redshift dependent factor $f_e(z) \equiv f_{IGM}(z)f_{ion}(z)$, where f_{ion} describes the effects of chemical composition and ionization state of the gas. For a primordial chemical composition and complete ionization $f_{ion} = 1$ by definition. In general the averaged electron concentration in the IGM can be expressed using $f_e(z)$ as:

$$\langle n_e \rangle (z) \equiv f_e(z)n_{e0}(1+z)^3 \quad (4)$$

It is convenient to rewrite Eq. 1 in the form, which separates the terms related to the concentration fluctuations from terms depending on the uniform cosmological model:

$$DM(z_S) = \int_0^{z_S} n_{e0} f_e(z) (1 + \delta_3) \frac{c/H_0 (1+z) dz}{h(z)} \quad (5)$$

where δ_3 is the 3D electron density fluctuation ($n_e = \langle n_e \rangle (z)(1 + \delta_3)$) - the only variable under the integral which depends on the spatial coordinates.

To employ the results of Illustris we imagine that our line of sight goes through several simulation cubes corresponding to different epochs (redshift ranges). The matter distribution is correlated on scales of tens of megaparsecs ([Geller et al. 1987](#)) and modeling the line of sight as a sum of sections, each belonging to a single cube takes these correlations into account. On the other hand there should be no strong correlations on larger scales and choosing at random photon paths through each cube guarantees that. For simplicity we consider photon paths parallel to one of the simulation cube edges, which saves programming and calculation time. (Compare [Carbone et al. 2008](#) about shifting and rotating simulation cubes at different epochs to get better approximation of statistical uniformity and isotropy of the simulated matter distribution.)

We construct a sequence of simulation cubes on the photon path using the condition:

$$\int_{z_{i-1}}^{z_i} (1+z) \frac{dl_{\text{prop}}}{dz} dz = \int_{z_{i-1}}^{z_i} \frac{c/H_0 dz}{h(z)} = 75 \text{ Mpc}/h \quad (6)$$

where the integral gives the comoving distance along the path. We start from $z_0 = 0$ and calculate the other z_i recursively. The redshift intervals corresponding to the photon travel through a single cube are small ($z_i - z_{i-1} \ll 1 + z_i$) so we can neglect the effects of cosmic expansion/evolution and use distribution of electrons given by δ_3 corresponding to the averaged redshift $z_{av,i} \equiv (z_{i-1} + z_i)/2$. Projecting the 3D distribution of the electron density fluctuations $\delta_3(z_{av,i})$ along one of the simulation cube edges we get the 2D distribution of the fluctuations in surface electron density $\delta_2(z_{av,i})$. The dispersion measure to a point at the redshift z_i can now be expressed as:

$$DM(z_i) = \sum_{j=1}^i (1 + \delta_2(z_{av,j})) \int_{z_{j-1}}^{z_j} n_{e0} f_e(z) \frac{(1+z)c/H_0 dz}{h(z)} \quad (7)$$

For other source redshifts we get $DM(z_S)$ by interpolation. The averaged dispersion measure $\langle DM(z_S) \rangle$ can be calculated by substituting $\delta_2(z_{av,j}) = 0$ into Eq. 7.

In Fig. 1 we show the redshift dependence of the dispersion measure in a model with uniform electron density and cosmological parameters corresponding to the Illustris simulation. The solid line shows the relation for averaged electron density in the IGM taken from Illustris (see the next subsection). The dashed line shows the dependence in a case, when all free electrons, regardless of their position relative to dark matter haloes, are included. Calculation with the same cosmological parameters but assuming $f_e(z) = 1$ gives the dotted line. The scatter in the dispersion measure σ_{DM} resulting from the nonuniform electron distribution is shown in the lower panel. For $z = 1$ we get $\sigma_{DM} = 115 \text{ pc cm}^{-3}$ about two times smaller than the result of [McQuinn \(2014\)](#) (his Fig. 1, lower panel) based on simulations. On the other hand our result based on the distribution of all electrons is in agreement with his value.

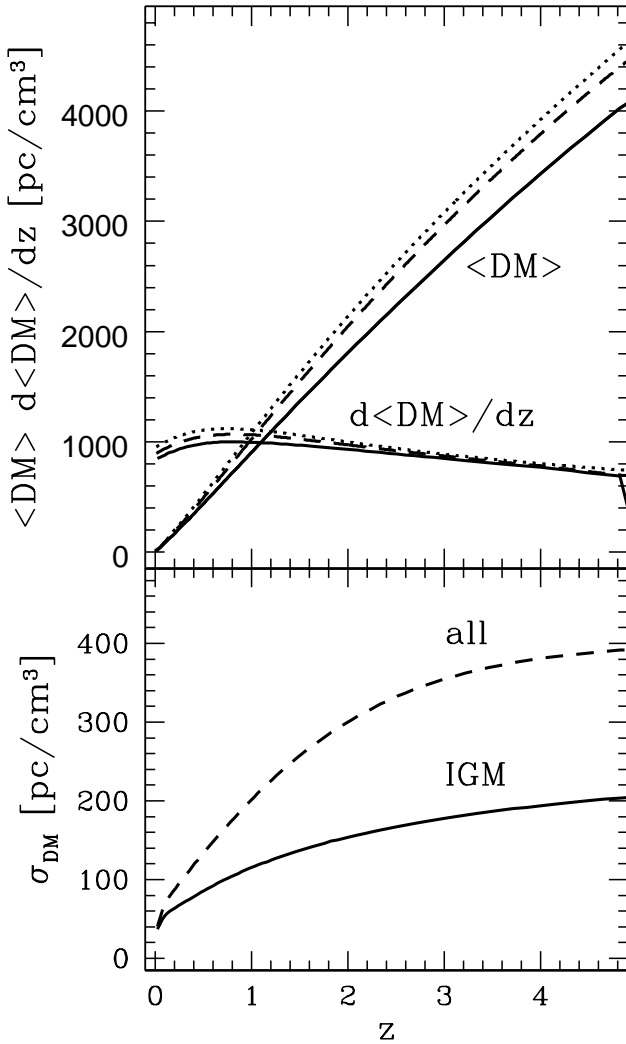


Figure 1. (Upper panel) The dependence of the averaged dispersion measure on the redshift and its derivative. Solid lines show the relations corresponding to the averaged electron density in the IGM alone taken from the Illustris simulation, the dashed lines take into account all free electrons according to Illustris, and the dotted lines are calculated under the assumption that all baryonic matter has the form of completely ionized gas with primordial composition. (Lower panel) The standard deviation of the dispersion measure is shown. Drawing conventions follow the upper panel

2.2 Distribution of ionized gas from Illustris simulation

We have downloaded the 3D maps of the distribution of matter in the Illustris-3 simulation cube corresponding to the epochs $z = 0, 0.5, 1, 2, 3, 4, 5, 5.5,$ and 6 . The simulation gives the positions, masses, densities, and ionization states of $\approx 455^3$ gas cells present at the beginning of calculations. Some of them become stars/wind particles during the evolution. The distribution of dark matter is given similarly as positions and masses of another 455^3 dark matter particles.

Haider et al. (2016) analyze large-scale mass distribution in the Illustris simulation, dividing the space into regions of voids, filaments, and haloes based on the local dark matter density. A region with $\rho_{DM} \geq 15\rho_c$ (dark matter density fifteen times higher than critical) is treated as belonging to a halo. The haloes occupy a tiny

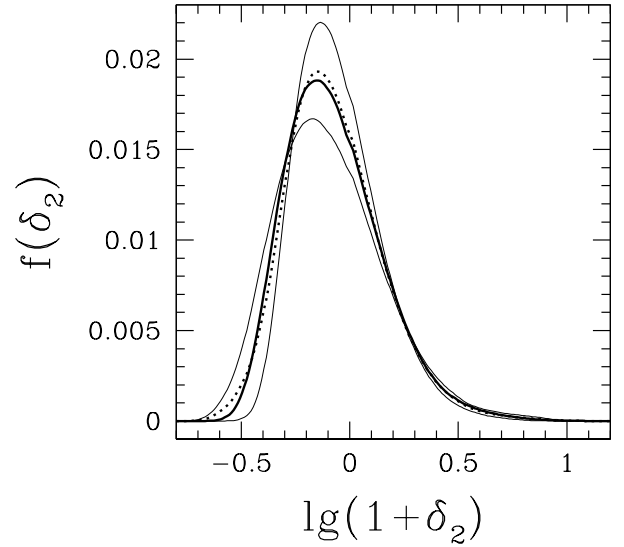


Figure 2. The probability distributions $f_{0.5}(\delta_2)$ (thick solid line), $f_0(\delta_2)$, $f_1(\delta_2)$ (thin solid lines), and interpolated distribution $f_{0.1}(\delta_2)$ (dotted) plotted as functions of $\lg(1 + \delta_2)$. See the text for details.

Table 1. Distribution of DM [pc cm^{-3}] for $z = 1, 2, 3, 4,$ and 5

z	$\langle DM \rangle$	σ_{DM}	γ_3	γ_4
1	905.	115.	0.64	3.79
2	1803.	154.	0.48	3.44
3	2649.	177.	0.39	3.30
4	3431.	194.	0.34	3.23
5	4136.	204.	0.31	3.19

fraction of the volume (0.16% today), but 49% of the dark matter and 23% of the baryons can be found there.

The 3D electron density fluctuations δ_3 are defined by the distribution of gas elements. Each gas cell has defined mass, mean density, and electron abundance, so their characteristic size and electron number can be calculated. The total mass density ρ at the position of a gas cell is also given. We use the criterion $\rho \geq 15\rho_c$ to distinguish gas elements belonging to haloes. Since the dark matter is overabundant in haloes and its density dominates anyway, this criterion is close to the one used by Haider et al. (2016). We neglect gas cells belonging to haloes when studying gas distribution in the IGM. We project the electron distribution onto three mutually perpendicular walls of the simulation cube, using top hat filter for each cell. We choose 2D maps of 16×16 k resolution. The pixel size ($\sim 5/h$ kpc) corresponds to the comoving size of the densest gas cells at $z = 0$. (All cells belonging to the IGM have much larger sizes.) The resulting maps of projected free electron distribution give probability distributions of 2D electron density fluctuations $f_z(\delta_2)$ based on 3×16384^2 "measurements" for chosen redshifts. By definition $\langle \delta_2 \rangle = 0$. We find the range of fluctuations on all considered maps to be $-0.86 \leq \delta_2 \leq 20.$. We use histograms with logarithmic bins of width 0.01 dex for storing and plotting probability distributions as functions of $-1 \leq \lg(1 + \delta_2) \leq 1.5$.

Using Illustris data we find the values of $f_{IGM}(z)$, $f_{ion}(z)$, and $f_e(z)$ for a set of redshifts (compare the upper part of Table 2). Almost all the baryons belong to the IGM at $z = 5$ (not shown in the Table) and then their fraction decreases monotonically to $f_{IGM} \approx 0.84$ at $z \approx 1$, to increase slightly at $z = 0$ due to the gas ejection from haloes. Since $z = 3$ IGM gas is almost completely

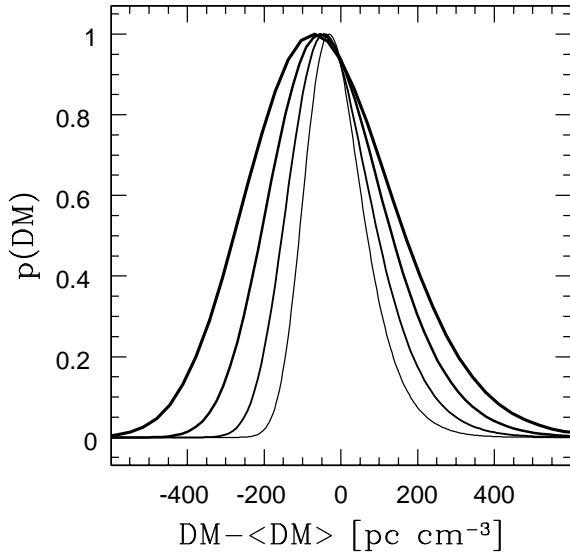


Figure 3. Probability distributions for the dispersion measures to sources at the redshifts $z \approx 0.5$ (thin line, narrow plot) 1, 2, and 4 (thick, wide). Values of $\langle DM \rangle(z)$ are given in Table 1.

ionized with $f_{ion} \geq 0.99$, so f_e is very close to f_{IGM} . At $z = 5$ $f_{ion} \approx 0.93$ due to incomplete helium ionization. The electron fraction parameter changes only by few per cent in the range $0 \leq z \leq 5$, and we linearly interpolate its value between $z = 0$ and $z = 1$, 1 and 2, etc where we know $f_e(z)$ based on Illustris data. At $z > 5$ electron concentration given by Illustris becomes nonphysically low and we do not exploit this range. On the other hand the results of Illustris for $2 < z < 4$ are in good agreement with the observations of Ly- α forest (Vogelsberger et al. 2014a) and there the data can be trusted. The plots of $d\langle DM \rangle/dz$ in Fig. 1 show the changes in Illustris electron density (solid line) as compared to the model assuming full ionization of all baryonic matter (dotted).

We approximate the probability distributions at any z interpolating between the distributions given by Illustris. For any z : $z_1 \leq z \leq z_2$ we assume

$$f_z(\delta_2) = \frac{z_2 - z}{z_2 - z_1} f_{z_1}(\delta_2) + \frac{z - z_1}{z_2 - z_1} f_{z_2}(\delta_2) \quad (8)$$

where $z_1 \in \{0, 1, 2, 3, 4\}$ and $z_2 = z_1 + 1$. We check our assumption comparing $f_{0.5}(\delta_2)$ based on Illustris data with interpolated $f_{0.1}(\delta_2) = 0.5 f_0(\delta_2) + 0.5 f_1(\delta_2)$. We show both distributions in Fig. 2. We also perform Kolmogorov-Smirnov test comparing the cumulative probability distributions:

$$F_z(\delta_2) = \int_{-\infty}^{\delta_2} f_z(x) dx \quad (9)$$

$$\max_{\delta_2} (|F_{0.1}(\delta_2) - F_{0.5}(\delta_2)|) = 0.0097 \text{ at } \delta_2 = -0.45 \quad (10)$$

The maximal difference between cumulative probability functions is much lower than the critical value of K-S test ($\sim 1/\sqrt{N}$) for $N = 250$ bins.

We have performed 10^8 trial simulation calculating dispersion measure for sources at the redshifts $0 < z_S < 5$, which in our approach corresponds to crossing up to 75 ($z_S \approx 5$) simulation cubes. The dispersion measure is calculated using Eq. 5 with δ_2 at each

cube chosen at random using probability distributions like these shown in Fig. 2.

The relative probability distributions of the simulated DM to sources at the chosen redshifts is shown in Fig. 3. In Table 1 we give the expected DM value expressed in units of pc cm^{-3} and its standard deviation σ_{DM} for chosen source redshifts. The values of higher moments of the probability distributions $\gamma_n \equiv \langle (DM - \langle DM \rangle)^n \rangle / \sigma_{DM}^n$ show that they are not far from being Gaussian (in which case $\gamma_3 = 0$ and $\gamma_4 = 3$).

3 SIMULATING FRBS OBSERVATIONS AND FITTING COSMOLOGICAL PARAMETERS

We simulate observations of FRBs with known redshifts. The source redshifts are drawn at random from the distribution $f(z) \propto z \exp(-z)$ (Zhou et al. 2014, Walters et al. 2018) limited to the range $0.5 \leq z \leq 4.5$. We also consider smaller redshift ranges $0.5 \leq z \leq 2.5$ and $0.5 \leq z \leq 1.5$. (The redshift distribution $f(z)$ describes gamma ray bursts (GRBs). We do not assume any physical relation between GRBs and FRBs. The difficulty in measuring redshifts for both kinds of phenomena may be similar, and FRBs may be related to stellar evolution as are GRBs. We use the distribution of observed redshifts of a known class of sources only as an example.)

Following Deng & Zhang (2014), Gao, Li & Zhang (2014) we assume, that the observations give the dispersion measure which is a sum of contributions from inter-galaxy medium, host galaxy, and our Galaxy:

$$DM_{obs} = DM_{IGM} + DM_{host} + DM_{Galaxy} \quad (11)$$

The contribution of our Galaxy to the dispersion measure can be estimated based on local measurements and subtracted from the observed value. As shown by simulations of Yang and Zhang (2016) the averaged value of the host galaxy contribution can be estimated based on observations of close FRBs. This result is based on the assumption that $\langle DM_{host} \rangle$ does not significantly evolve which implies its $\propto 1/(1+z)$ contribution to DM_{obs} , while for the IGM part we have roughly $\langle DM_{IGM} \rangle \propto z$ (compare Fig. 1, Table 1). Different redshift dependencies allow fits of both parts for a large enough sample of close bursts. In the following we assume, that the average host contribution can be subtracted from the observed DM , giving the approximate value of the IGM part:

$$DM_{IGM,obs} = DM_{obs} - \langle DM_{host} \rangle / (1+z) - DM_{Galaxy} \quad (12)$$

According to Tendulkar et al. (2017), who analyze the repeating FRB 121102 and Yang et al. (2017), who statistically investigate 21 FRBs, the value of DM_{host} is high ($\geq 200 \text{ pc cm}^{-3}$) and has large scatter. Following Yang and Zhang (2016), Walters et al. (2018) we assume DM_{host} to have normal distribution. We adopt the value $\sigma_{host} = 50 \text{ pc cm}^{-3}$ for its standard deviation. Thus our simulated $DM(z_k)$, which represents its IGM part after subtracting the Galaxy and averaged host contributions, includes also an extra term which is normally distributed:

$$DM_k = DM(z_k) + \sigma_h(z_k) * \mathcal{N}(0, 1) \quad (13)$$

$$\sigma_h(z_k) = \sigma_{host} / (1+z_k) \quad (14)$$

where $DM(z_k)$ is given by Eq. 7 and $\mathcal{N}(0, 1)$ is the normal distribution with zero mean and unit variance.

We fit model parameters denoted Θ looking for the minimum

Table 2. Electron fraction parameters

		Illustris				
z		0	1	2	3	4
f_{IGM}		0.847	0.841	0.876	0.928	0.964
f_{ion}		0.993	0.992	0.992	0.990	0.979
f_e		0.841	0.835	0.869	0.918	0.944
		Fits to f_e				
100	4.5	.83±.10	.83±.09	.87±.11	.92±.17	.99±.32
400	4.5	.83±.05	.83±.04	.86±.06	.90±.08	.98±.14
100	2.5	.83±.07	.83±.06	.87±.08		
100	1.5	.83±.07	.83±.07	.87±.50		
σ_{mod}		.008	.010	.011	.008	.012

of

$$\chi_{FRB}^2 = \sum_k \frac{(DM_k - DM_0(z_k; \Theta))^2}{\sigma_k^2 + \sigma_h^2(z_k)} \quad (15)$$

which is a standard approach. $DM_0(z_k; \Theta)$ is a model prediction of the dispersion measure to the source at the redshift z_k . Despite the fact that the distribution of simulated DM_k is only weakly non-Gaussian, we always investigate the distribution of calculated χ^2 and set its critical value χ_{crit}^2 such that in 95% of cases $\chi^2 \leq \chi_{crit}^2$. We accept fits with χ^2 values below critical.

Illustris gives the concentration of electrons in space and its time dependence for a single realization of simulations performed in a cosmological model with given set of parameters. We do not have similar information based on simulations for other universe models. The scenarios of gravitational instability and reionization influence the distribution of electrons in a complicated way specific to each model. Results of Illustris show, that the fraction of baryons in the IGM changes with time and ionization is incomplete at early epochs so working under the simplifying assumptions of $f_e \approx 1$ one would systematically overestimate model values of DM . Thus introduction of at least one parameter describing the free electron fraction seems necessary. The FRBs tests to find $\Omega_B f_e$ has been proposed by [Deng & Zhang \(2014\)](#). [Shull & Danforth \(2018\)](#) propose calibration of the fraction of baryons in the diffuse IGM. We follow these ideas checking the possibility of estimating the free electron fraction in the IGM and its dependence on the redshift.

First we check whether it is possible to recover the values of $f_e(z_i)$ ($z_i = 0, 1, 2, 3, 4$) used in simulations and given in the upper part of Table 2 assuming other model parameters ($H_0, \Omega_M, \Omega_\Lambda, \Omega_B$) to have the values used in Illustris. (When dealing with real data one would use their current *precision cosmology* values.) Since $DM_0(z_k; \Theta)$ can be expressed as a linear combination of $f_e(z_i)$ the minimization of χ_{FRB}^2 becomes a *linear least squares* problem solvable with standard methods of the linear algebra. Using our methods we generate many samples of simulated FRBs drawing their redshifts from the assumed distribution and use the range $0.5 \leq z_k \leq 4.5$ with $1 \leq k \leq N$. For $N = 100$ we encounter numerical problems (“singular matrix”) in less than one case per million. For any simulated sample the fitted parameters may be unphysical ($f_e < 0$) which is rare and in practice happens only for $f_e(z = 4)$ or have excessive values $f_e > 1$. The latter occurs when sources belonging to a sample happen to lie behind over-dense regions of space. On average the fitted f_e values reproduce their simulation counterparts. Their standard deviations depend on the sample size N in usual way $\propto 1/\sqrt{N}$ - compare Table 2, but are rather high. Averaged electron density for $0 \leq z \leq 1$ depends on $f_e(z = 0)$ and $f_e(z = 1)$ in our approach and these two parameters influence the expected dispersion measure for all sources in a sample, while

$f_e(z = 4)$ has an impact only on sources with $z_k \geq 3$, which are less numerous (0.22 N on average). Thus the estimate of f_e at higher redshifts has a larger standard deviation.

Using samples with smaller redshift range ($0.5 \leq z \leq 2.5$, $0.5 \leq z \leq 1.5$) we try to fit the electron fraction parameters for $z = 0, 1$, and 2. In the first case the fits are as good as for samples with larger redshift ranges, but in the latter case $f_e(z = 2)$ is practically unconstrained despite the fact that the expected values of DM for all sources at $z > 1$ do depend on this parameter. Examining Table 2 one can see that to fit f_e with the accuracy of one per cent samples with $N \sim 10^4$ are needed.

In the analysis above we have neglected the uncertainty resulting from using wrong values of cosmological model parameters when fitting $f_e(z_i)$. We assume four parameters p_i ($p_i \in \{H_0, \Omega_B, \Omega_M, \Omega_\Lambda\}$) to have values known from other studies with errors σ_i . Neglecting correlations between p_i we would get:

$$\sigma_{model}^2 = \sum_{i=1}^4 \left(\frac{\partial f_e}{\partial p_i} \right)^2 \sigma_i^2 \quad (16)$$

The recent estimates of cosmological parameters are given in Planck Results 2018 ([Aghanim et al. 2018](#)). According to this study H_0 is weakly anti-correlated with Ω_B . On the other hand the measured quantity $DM \propto f_e * \Omega_B * H_0$ (compare Eqs. 3, 5), so Eq. 16 overestimates uncertainty resulting from errors in these two parameters. The universe model is practically flat (ibid.) so Ω_M and Ω_Λ are strictly anti-correlated. We examine the influence of their values on electron fractions by repeating calculations for $\Omega_M = \Omega_{MI} + \Delta$ and $\Omega_\Lambda = \Omega_{\Lambda I} - \Delta$, where $\Delta = \sigma_{\Omega_M} = \sigma_{\Omega_\Lambda}$. We add the estimated uncertainty in quadrature to uncertainties from the other two parameters getting values shown in the last row of Table 2. Because we have neglected the weak anti-correlation between H_0 and Ω_B the numbers in the table should be treated as upper limits. This shows that the uncertainty of fitted electron fractions resulting from the uncertainty of the used *precision cosmology* model is of the order of one per cent.

Next we check the possibility of testing both the electron fraction and the geometry of the universe model using FRBs. Since the dispersion measure is directly proportional to the product of f_e, H_0 , and Ω_B (Eqs. 3,5) placing any limits on these parameters separately is impossible. We simplify our approach looking only for the expected electron fraction assuming H_0 and Ω_B to be known independently. The dispersion measure to source at a given redshift z_S depends on the electron fraction in the redshift interval $0 \leq z \leq z_S$ in proportion to

$$\langle f_e \rangle(z_S) = \frac{\int_0^{z_S} f_e(z) \frac{(1+z)dz}{h(z)}}{\int_0^{z_S} \frac{(1+z)dz}{h(z)}} \quad (17)$$

The averaged electron fraction $\langle f_e \rangle$ is slowly and monotonically changing from 0.825 at $z = 0.5$ to 0.845 at $z = 4.5$. Averaging over the source redshift distribution

$$\langle \langle f_e \rangle \rangle = \frac{\int_{z_{min}}^{z_{max}} \langle f_e \rangle(z_S) f(z_S) dz_S}{\int_{z_{min}}^{z_{max}} f(z_S) dz_S} \quad (18)$$

we get the expected $\langle \langle f_e \rangle \rangle$ values which are almost the same for the three ranges of sources redshifts considered (see Table 3).

Despite simplifications we have been unable to place any interesting constraints on Λ CDM model with three free parameters ($\Omega_M, \Omega_\Lambda, f_e$). The fits give large and irregular confidence regions with a substantial fraction of solutions grouped near the boundaries of the considered parameters region. (We limit the possible val-

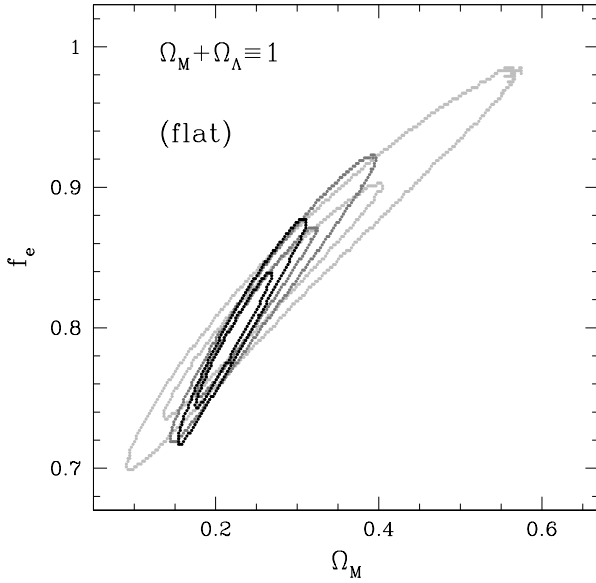


Figure 4. Distribution of fits to a flat Λ CDM model. Three redshift ranges ($0.5 \leq z \leq 4.5$ - black; $0.5 \leq z \leq 2.5$ - dark gray; $0.5 \leq z \leq 1.5$ - light gray) of the FRBs have been considered. The 68% and 95% confidence regions are shown, based on $\sim 4 \times 10^6$ simulated FRBs samples for each redshift range.

Table 3. Fits to flat Λ CDM models

N	z_{max}	Ω_M	f_e	f'_e	$\langle\langle f_e \rangle\rangle$
100	4.5	0.23 ± 0.03	0.80 ± 0.03	0.842 ± 0.008	0.847
100	2.5	0.26 ± 0.05	0.82 ± 0.04	0.833 ± 0.009	0.841
100	1.5	0.29 ± 0.10	0.83 ± 0.06	0.829 ± 0.010	0.838

ues of the parameters to $\Omega_{BI} \leq \Omega_M \leq \Omega_{BI} + 1$, $0.3 \leq \Omega_\Lambda \leq 1.3$, $0.3 \leq f_e \leq 1.3$.)

We show the results for flat Λ CDM models in Fig. 4 and in Table 3. We have considered three ranges of FRBs redshifts in our simulations ($0.5 \leq z_S \leq 4.5$, $0.5 \leq z_S \leq 2.5$, and $0.5 \leq z_S \leq 1.5$). In each case we have simulated 4×10^6 “observed” FRBs samples. For each sample we have fitted a flat Λ CDM cosmological model. We have obtained histograms of fitted parameter values $N(\Omega_M, f_e)$ for various ranges of source redshifts. We find, that even a wide redshift range of FRBs ($0.5 \leq z_S \leq 4.5$) gives only a rough estimate of parameters. The fitted Ω_M and f_e are strongly correlated with $\rho \approx 0.97$. The averaged result of many fits depends on the sample’s redshift range and is biased.

Fixing both density parameters ($\Omega_M = \Omega_{MI}$, $\Omega_\Lambda = \Omega_{\Lambda I}$) we get estimates of sample averaged electron fraction, which we denote f'_e in Table 3. Their values agree with the analytical prediction $\langle\langle f_e \rangle\rangle$. This shows that in a fixed cosmological model one can get the redshift and sample averaged electron fraction with the uncertainty of \sim two per cent using a sample of one hundred FRBs (plus one per cent uncertainty of the model).

4 TESTS BASED ON FRBS AND OTHER DATA

Limited possibilities of FRBs tests suggest to use also some other data to make useful constrains on the models, obtaining at least

Table 4. Fits of Λ CDM and electron fraction models to combined synthetic samples of SN’*e* and FRBs

model	z_{max}	Ω_M	Ω_Λ	f_e
Illustris		0.2726	0.7274	
SN		0.345 ± 0.099	0.863 ± 0.245	
SN’ & FRBs	4.5	0.20 ± 0.03	0.64 ± 0.06	0.832 ± 0.013
SN’ & FRBs	2.5	0.24 ± 0.06	0.70 ± 0.09	0.831 ± 0.013
SN’ & FRBs	1.5	0.28 ± 0.09	0.74 ± 0.12	0.828 ± 0.014
SN’ & FRBs flat	4.5	0.254 ± 0.013	$1 - \Omega_M$	0.825 ± 0.013

cosmological density parameters and electron fraction simultaneously.

As an example we combine simulated FRBs and SNe Ia samples. We use the SCP “Union” SN Ia data (Kowalski et al. 2008) as a basis of obtaining our synthetic samples. The “Union” sample contains 307 *usable* lightcurves. We have downloaded the data in the form $\{z_j, \mu_j, \sigma_j\}$ redshift – distance modulus – its estimated error. The best fit of a Λ CDM model to the real SNe Ia data gives cosmological parameters which are within 1-sigma from Illustris parameters but are different. To check whether our tests reproduce cosmological parameters used in simulations we replace the “Union” SN Ia data by synthetic samples SN’ with the same redshifts and estimated errors but *corrected* distance moduli: μ'_j with Gaussian noise:

$$\mu'_j = 5 \lg \left(\frac{d_L(z_j; \Omega_M, \Omega_\Lambda)}{10 \text{ pc}} \right) + \sigma_j \mathcal{N}(0, 1) \quad (19)$$

where d_L is the luminosity distance and Illustris cosmology parameters are used.

We consider Λ CDM models with two free parameters (Ω_M and Ω_Λ) while the Hubble constant and baryon density are fixed at Illustris values. The averaged electron fraction f_e , which does not influence the geometry of the universe model or the SN’ data fits, is necessary to model FRBs. The SN’ part of the χ^2 reads:

$$\chi^2_{SN} = \sum_{j=1}^{307} \frac{(\mu'_j - \mu_0(z_j; \Omega_M, \Omega_\Lambda))^2}{\sigma_j^2} \quad (20)$$

$$\mu_0(z_j; \Omega_M, \Omega_\Lambda) = 5 \lg \left(\frac{d_L(z_j; \Omega_M, \Omega_\Lambda)}{10 \text{ pc}} \right) \quad (21)$$

where μ_0 is a model predicted distance modulus.

Now we look for cosmological parameters which minimize χ^2 for a combined FRB plus SN’ data. For each FRB and SN’ data simulation we find the minimum of:

$$\chi^2 = \chi^2_{FRB}(\Omega_M, \Omega_\Lambda, f_e) + \chi^2_{SN}(\Omega_M, \Omega_\Lambda) \quad (22)$$

Since there are 307 SN Ia in the SN Union sample, we use simulated FRBs data samples consisting of 300 sources each. We examine many combined sets. In Fig. 5 we show confidence regions for Ω_M , Ω_Λ , and sample averaged f_e projected into two or one dimension. Table 4 gives the fitted parameter values with 1D 68% confidence regions.

The tests based on combined data allow to constrain both cosmological density parameters (Ω_M , Ω_Λ) but their accuracy is still far from the present *precision cosmology* standards. On the other hand our simulation shows that using few hundred of FRBs with another moderate precision test one is able to measure the averaged electron fraction with uncertainty of \sim two per cent.

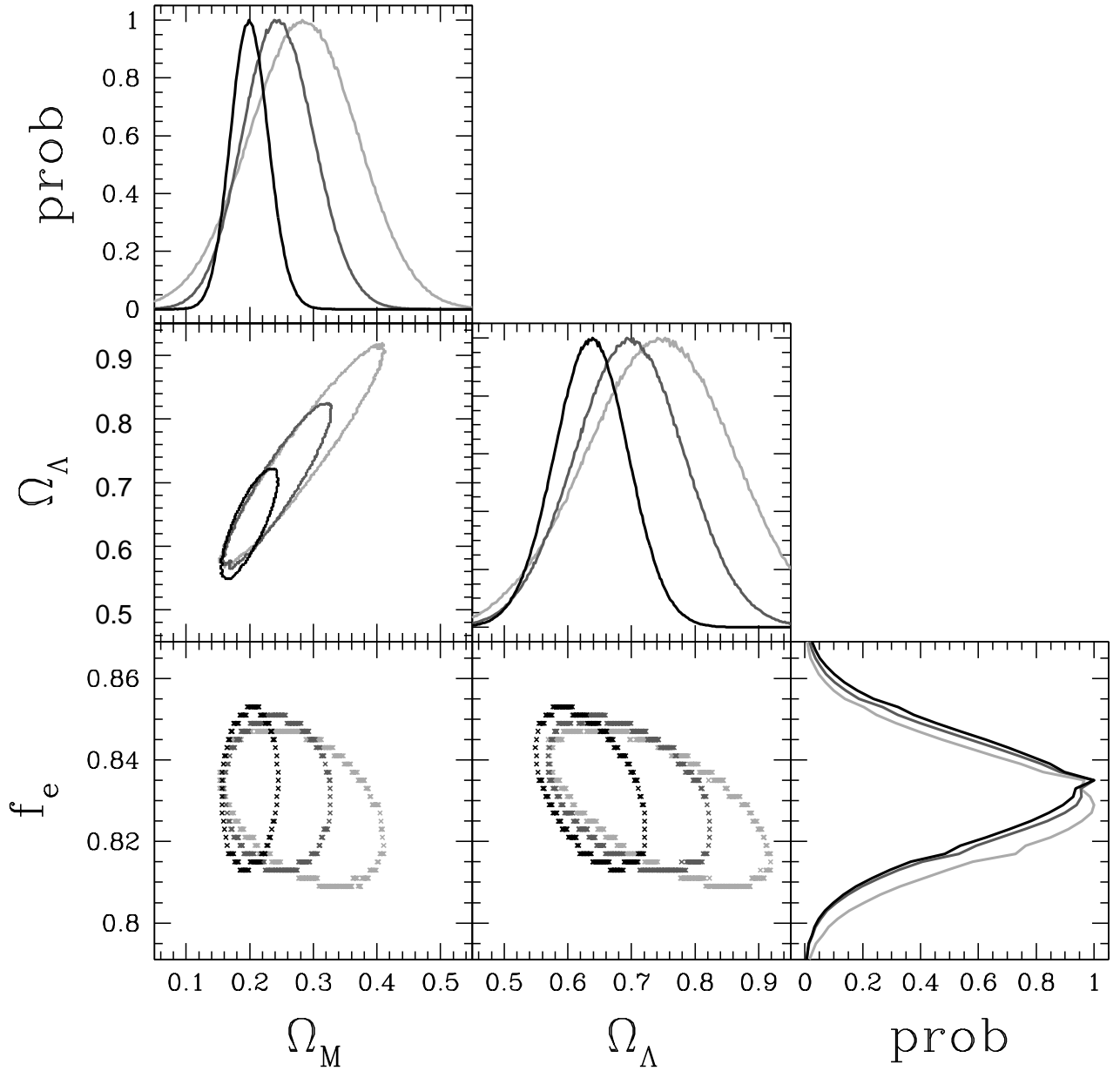


Figure 5. Confidence regions for Λ CDM model parameters and averaged electron fraction based on combined data (synthetic SN^I Ia samples and our simulated FRBs samples). We plot boundaries of regions of 68% confidence level. Results for the samples with the largest redshift range ($0.5 \leq z_S \leq 4.5$) are plotted with black lines, for $0.5 \leq z_S \leq 2.5$ - dark gray, and for $0.5 \leq z_S \leq 1.5$ - light gray.

5 DISCUSSION

We have analyzed the evolution of the distribution of ionized gas in the IGM using the results of the Illustris simulation (Vogelsberger et al. 2014a,b). According to our calculations the fraction of gas in the IGM changes from $f_{IGM} \approx 1$ at $z = 5$ to 0.85 at $z = 0$. This result is different from Haider et al. (2016), who obtain $f_{IGM} \approx 0.77$ at $z = 0$. For $z < 3$ the IGM gas is almost completely ionized, and free electron fraction $f_e \approx f_{IGM}$. The estimate of Shull & Danforth (2018) who claim that the diffuse baryons constitute 0.6 ± 0.1 of all gas is based on different reasoning.

The spatial distribution of ionized gas and its evolution given by Illustris allows us to simulate calculations of the dispersion measure along any LOS and obtain its standard deviation as a function of the source redshift. Our results on averaged DM to a source at given redshift (Fig. 1, Table 1) are in rough agreement with other authors (e.g. Zhou et al. 2014, Deng & Zhang 2014), and with the approximate formula of Zhang (2018):

$$DM_{IGM} \approx 855 \text{ pc cm}^{-3} z \quad (23)$$

At $z = 1$ we get σ_{DM} which is about two times lower as compared to the results of McQuinn (2014) based on simulations. Only if all gas

from Illustris except *stellar cells* is included in calculations we get the agreement with his $\sigma_{DM}(z=1)$ value. The shape of our $\sigma_{DM}(z)$ dependence is different and resembles his analytical results.

The dispersion measure to a given source is directly proportional to the density of free electrons along LOS. In our approach we model it using the electron fraction parameter $f_e(z)$ (Eq. 4). In simulations we use its values at $z=0, 1, \dots, 5$ and linearly interpolate between them. Following [Deng & Zhang \(2014\)](#), [Shull & Danforth \(2018\)](#) and others we check the possibility of finding the history of ionization using a sample of observed FRBs and assuming cosmological parameters ($H_0, \Omega_B, \Omega_M, \Omega_\Lambda$) to be known exactly. We show, that to get the the dependence of the electron fraction on the redshift with one per cent accuracy, samples of $N \sim 10^4$ events are needed (compare Table 2). The present errors in cosmological parameters values (e.g. [Aghanim et al. 2018](#)) introduce another one per cent uncertainty. On the other hand the redshift and sample averaged electron fraction can be constrained with accuracy better than two per cent based on $N = 100$ FRBs in a fixed cosmological model (compare Table 3). The dependence on cosmological parameter errors is the same as above.

We have shown, that using a sample of three hundred FRBs and a sample resembling SN Ia Union Sample ([Kowalski et al. 2008](#)) we are able to constrain the averaged electron fraction parameter with the accuracy of \sim two per cent (compare Table 4).

The cosmological tests based on large future samples of FRBs are possible, but are unlikely to give the accuracy of the present day precision cosmology. This conclusion with more details has already been reached by [Walters et al. \(2018\)](#). There are degeneracies between derived universe model parameters, which can be removed only by using other type of data, as shown by our consideration of joint FRBs and SN Ia tests. The observations of FRBs with measured redshifts may give valuable data on the distribution of free electrons in space also on cosmological scales (compare [Shull & Danforth 2018](#)). Since the dispersion measure depends on the electron distribution between the source and the observer, the dependence of the electron fraction on the redshift can, at least in principle, be investigated. In this aspect samples of FRBs with known redshifts may be a better target than Cosmic Microwave Background observations yielding Thompson optical depth τ_e and Suniajev-Zeldovich y parameter characterizing the electron population between the observer and the Last Scattering Surface (see e.g. [Aghanim et al. 2018](#)).

ACKNOWLEDGMENTS

We thank the Anonymous Referee for his constructive comments, which helped to improve the paper. The Illustris Simulation databases used in this paper and the web application providing online access to them were constructed as part of the activities of the German Astrophysical Virtual Observatory.

REFERENCES

- Aghanim, N. et al. (Planck Collaboration), 2018, arXiv:1807.06209
- Ando, S., Nagai, D., 2012, J. Cosmology Astropart. Phys., 07, 017
- Bilous, A.V. et al., 2016, A&A, 591, 134
- Carbone, C., Springel, V., Baccigalupi, C., Bartelmann, M., Matarrese, S., 2008, MNRAS, 388, 1618
- Chatterjee, S. et al., 2017, Nature, 541, 58
- Deng, W., Zhang, B., 2014, ApJ, 783, L35
- Dolag, K., Gaensler, B.M., Beck, A.M., Beck, M.C., 2015, MNRAS, 451, 4277
- Gao, H., Li, Z., Zhang, B., 2014, ApJ, 788, 189
- Geller, M.J., Huchra, J.P., de Lapparent, V., 1987, in: *Observational cosmology; Proceedings of the IAU Symposium, Beijing*, Dordrecht, D. Reidel Publishing Co, p. 301
- Haider, M. et al., 2016, MNRAS, 457, 3024
- Kaiser, N., Squires, G., 1993, ApJ, 404, 441
- Katz, J.I., 2017, MNRAS, 472, L85
- Kowalski, M. et al., 2008, ApJ, 686, 749
- Lorimer, D.R., Bailes, M., McLaughlin, M.A., Narkevic, D.J., Crawford, F., 2007, Science, 318, 777
- Lorimer, D., 2016, Nature, 530, 427
- McQuinn, M., 2014, ApJ, 780, L33
- Nelson, D., Pillepich, A., Genel, S., Vogelsberger, M., Springel, V., Torrey, P., Rodriguez-Gomez, V., Sijacki, D., Snyder, G.F., Griffen, B., Marinacci, F., Blecha, L., 2015, Astron.Comp., 12
- Paczynski, B., 1995, PASP, 107, 1167
- Ravi, V., 2017, arXiv:1710.08026
- Schneider, P. 2005, in: *Kochanek, C.S., Schneider, P., Wambsganss, J.: Gravitational Lensing: Strong, Weak & Micro*. G. Meylan, P. Jetzer & P. North (eds.), Springer-Verlag: Berlin, p.273
- Shull, J.M., Danforth, Ch.W., 2018, ApJ, 852, L11
- Tendulkar, S.P., et al., 2017, ApJ, 834, L7
- Vogelsberger, M., Genel, S., Springel, V., Torrey, P., Sijacki, D., Xu, D., Snyder, G., Bird, S., Nelson, D., Hernquist, L., 2014, Nature, 509, 177
- Vogelsberger, M., Genel, S., Springel, V., Torrey, P., Sijacki, D., Xu, D., Snyder, G., Bird, S., Nelson, D., Hernquist, L., 2014, MNRAS, 444, 1518
- Walters, A., Weltman, A., Gaensler, B.M., Ma, Y.Z., Witzemann, A., 2018, ApJ, 856, 65
- Yang, Y.-P., Luo, R., Li, Z., Zhang, B., 2017, ApJ, 839, L25
- Yang, Y.-P., Zhang, B., 2016, ApJ, 830, L31
- Yu, H., Wang, F.Y., 2017, A&A, 606, 3
- Zhang, B., 2018, ApJ, 867, L21
- Zhou, B., Li, X., Wang, T., Fan, Y.-Z., Wei, D.-M., 2014, Phys. Rev. D, 89, 107303